American Mineralogist, Volume 96, pages 820–827, 2011

In situ determination of the spinel–post-spinel transition in Fe_3O_4 at high pressure and temperature by synchrotron X-ray diffraction

K. Schollenbruch,[1,*] A.B. Woodland,[1] D.J. Frost,[2] Y. Wang,[3] T. Sanehira,[3] and F. Langenhorst[2]

[1]Institut für Geowissenschaften, Universität Frankfurt, 60438 Frankfurt, Germany
[2]Bayerisches Geoinstitut, Universität Bayreuth, 94550 Bayreuth, Germany
[3]Center for Advanced Radiation Sources, The University of Chicago, 5640 S. Ellis Avenue, Chicago, Illinois 60637, U.S.A.

Abstract

The position of the spinel–post-spinel phase transition in Fe_3O_4 has been determined in pressure-temperature space by in situ measurements using a multi-anvil press combined with white synchrotron radiation. Pressure measurement using the equation of state for MgO permitted pressure changes to be monitored at high temperature. The phase boundary was determined by the first appearance of diffraction peaks of the high-pressure polymorph (h-Fe_3O_4) during pressure increase and the disappearance of these peaks on pressure decrease along several isotherms. We intersected the phase boundary over the temperature interval of 700–1400 °C. The boundary is linear and nearly isobaric, with a slightly positive slope.

Post-experiment investigation by TEM confirms that the reverse reaction from h-Fe_3O_4 to magnetite during decompression leads to the formation of microtwins on the (311) plane in the newly formed magnetite. Observations made during the phase transition suggest that the transition has a pseudomartensitic character, explaining in part why magnetite persists at conditions well within the stability field of h-Fe_3O_4, even at high temperatures. This study emphasizes the utility of studying phase transitions in situ at simultaneously high temperatures and pressures since the reaction kinetics may not be favorable at room temperature.

Keywords: Magnetite, post-spinel, phase transition, synchrotron experiment

Introduction

Magnetite ($FeFe_2O_4$) belongs to the large group of spinel-structured minerals with the general formula AB_2O_4. It is an important accessory mineral in many magmatic and metamorphic rocks and occurs as a component in spinels of the spinel peridotite facies of the upper mantle (e.g., Wood and Virgo 1989), as well as in $(Mg,Fe)_2SiO_4$ ringwoodite, which is expected to be stable in the mantle transition zone (e.g., O'Neill et al. 1993). Nearly pure magnetite has also been found as inclusions in diamonds (Meyer 1987; Stachel et al. 1998). Hence the stability and high-pressure properties of Fe_3O_4 have direct relevance to geochemical processes in the deep earth as magnetite and its polymorphs provide important structural models for understanding the behavior of Fe^{3+}-bearing components in the mantle. Further knowledge about its high-pressure behavior is fundamental for the understanding of the phase relations in the simple Fe-O system. For these reasons, magnetite has been the subject of many studies over the years. Magnetite is known to undergo an unquenchable phase transition at ~21 GPa at room temperature to a high-pressure polymorph (hereafter denoted as h-Fe_3O_4) (Mao et al. 1974; Huang and Bassett 1986; Pasternak et al. 1994; Fei et al. 1999). The h-Fe_3O_4 polymorph was found by Fei et al. (1999) to have space group *Pbcm* ($CaMn_2O_4$-type structure) with cell parameters a = 2.7992(3), b = 9.4097(15), and c = 9.4832(9) Å at 24 GPa and 650 °C. However, more recent studies suggest that a $CaTi_2O_4$-type structure (with space group *Bbmm*) is more consistent with the available diffraction data from room-temperature experiments between 21.8 and 43 GPa (Haavik et al. 2000) or experiments up to 930 °C and 60 GPa (Dubrovinsky et al. 2003). The unquenchable nature of h-Fe_3O_4 complicates direct crystallographic analysis of this phase. A further difficulty in studying this transition is the apparent sluggishness of the reaction and the persistence of magnetite at pressures significantly above that where h-Fe_3O_4 first appears (e.g., Huang and Bassett 1986). In addition, there is a large hysteresis in the back-reaction to magnetite, even at temperatures up to ~800 °C (e.g., Huang and Bassett 1986; Woodland et al. 2001). For these reasons, the actual position and slope of the phase boundary in *P-T* space remains poorly constrained. In this contribution we report the results of in situ diffraction measurements at high pressures and temperatures using synchrotron radiation that provide further important constraints on the position of the magnetite–h-Fe_3O_4 phase boundary. Our new experiments significantly expand the temperature range investigated by earlier studies. The current

* E-mail: schollenbruch@em.uni-frankfurt.de

results are consistent with our recent electrical resistivity study (Schollenbruch et al. 2009), but provide a more definitive delineation of the boundary.

Experimental methods

Magnetite starting material was produced by sintering Fe_2O_3 powder in a gas mixing furnace at one atmosphere, 1300 °C and log $f_{O_2} = -5.5$. Under these conditions the magnetite should be essentially stoichiometric (Dieckmann 1982). X-ray diffraction analysis revealed single-phase magnetite with a unit-cell parameter of a_o = 8.3966(6) Å, which is in good agreement with that of Haavik et al. (2000).

High-pressure, high-temperature experiments were performed using the GSECARS online multi-anvil press at beamline 13-ID-D at the Advanced Photon Source at Argonne National Laboratory, U.S.A. The 1000 t Kawai-type multi-anvil press and the beamline setup are described in detail by Wang et al. (1998, 2009). A major advantage of using a multi-anvil press combined with synchrotron radiation is that pressure can be monitored during the experiment by measuring the unit-cell parameter of a standard material located next to the sample. In conventional laboratory multi-anvil experiments, pressure determination is based on a series of calibrations at both room temperature and high temperature, using electrical resistance or quenchable phase transitions as pressure markers (the so-called fixed points). These calibrations typically are performed such that the sample is pressurized to the target pressure prior to heating (such as paths A and A′ in Fig. 1). In reality, the pressures achieved at high temperature are path dependent, hence it is difficult to intersect a phase boundary that has a weak temperature dependence, based on fixed point pressure calibration. With an online multi-anvil press, the pressure can be varied (and monitored) during the experiment, even at high temperatures, permitting other *P-T* trajectories to be explored (e.g., paths B or B′ in Fig. 1).

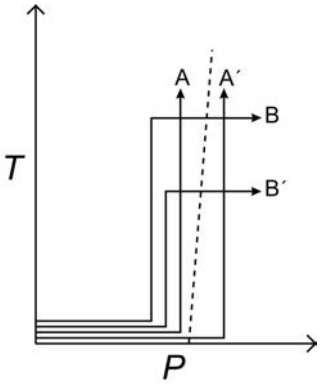

Figure 1. Problem of determination of a near-isobaric phase boundary (dashed line) with a conventional MA-apparatus (A, A´), where pressurization is followed by heating. To cross such a phase boundary at a high-angle, pressure-temperature profiles like B-B´ are required.

Each sample was pressed to a ~1 mm long cylinder and placed in a COMPRES 10/5 (octahedral edge length/truncation edge length in millimeters) standard pressure assembly (Fig. 2). The pressure cell has a Re foil furnace, surrounded by a $LaCrO_3$ sleeve (Leinenweber, p.c.). Slits in the sleeve and Re foil filled with B-epoxy plugs provided a window for the incident and diffracted radiation, which was detected by an energy-dispersive Ge solid-state detector located at a fixed diffraction angle of 6.1° (Wang et al. 2009). Both the height and width of the incident beam were 0.1 mm. On the diffraction side, the beam height was 0.1 mm and the beam width 0.3 mm. The sample diameter was about 1.5 mm. The geometry of the sample with respect to the synchrotron beam is illustrated in Figure 2.

Temperature was monitored by a $W_{74}Re_{26}/W_{95}Re_5$ thermocouple, without correcting the effects of pressure on the emf. The magnetite sample was packed in an MgO sleeve to separate it from the furnace. Approximately half of the available sample chamber volume was used for a mixture of fine-grained MgO and Pt or Au powder (mixing ratio 30:1), which served as pressure standard. The equation of state (EoS) for MgO from Dewaele et al. (2000) and those for Pt given by Jamieson et al. (1982) were used to convert the molar volumes of these phases obtained from diffraction patterns into working pressures. Values derived from the equations of state of MgO and Pt are in good agreement with each other, with a maximum deviation of 1 GPa. Differences between the two calibrations are not systematic, however, pressures derived from the Pt EoS tended to be more variable. For this reason, all pressures quoted here are based on the EoS of MgO.

Before each experiment, the 2θ angle was calibrated using an α-Al_2O_3 diffraction standard (Formal NBS XRD intensity standard 674a). Energy-dispersive diffraction patterns were obtained during the experiments and were analyzed by LeBail refinement using the GSAS software package (Larson and von Dreele 1988) and the EXPGUI interface of Toby (2001). An imaging system was used to help position the sample and pressure standards with respect to the incident beam, allowing accurate tracking of the sample position during the course of the experiment (i.e., after changing temperature or pressure). This assured that the diffraction patterns were acquired from the central region of either the sample or the pressure standards. The diffraction and imaging setups can be quickly switched back and forth. The experiments were performed between room temperature and 1400 °C and pressures up to 16 GPa (Table 1). After the experiments, the samples were recovered and prepared as polished sections for investigations by microprobe

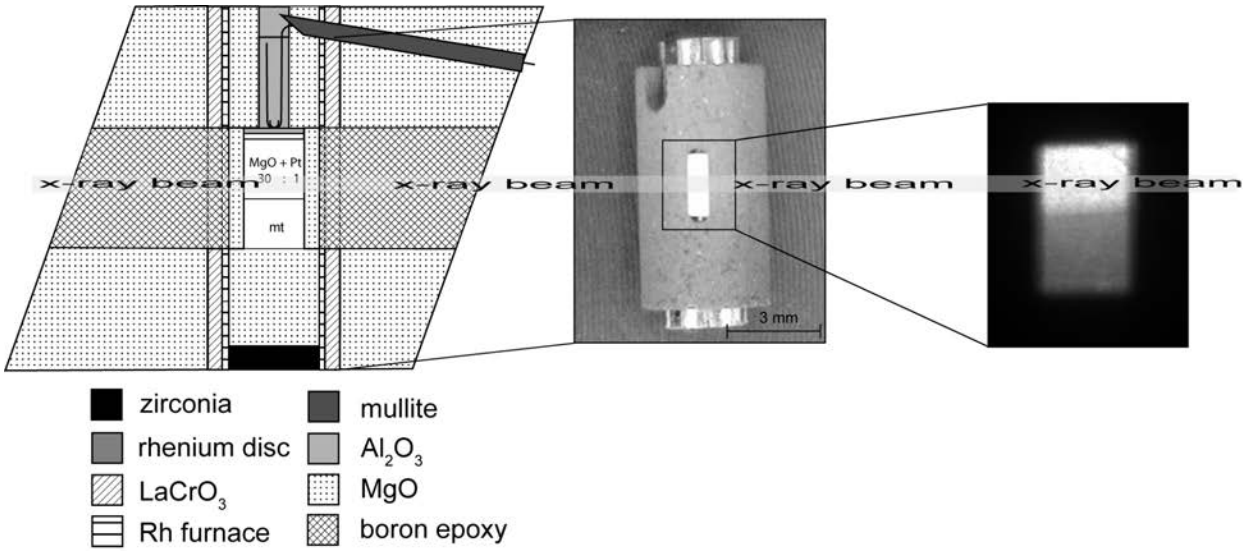

Figure 2. Schematic sketch of the COMPRES 10/5 pressure cell with a picture of the inner part of the cell and an X-ray radiographic image of the pressure medium and the sample.

TABLE 1. Range of *P* and *T* of the different in situ experiments

Experiment	Temperature (°C)	Pressure (GPa)
T0930	800	~9
	1200	10
	1000	9–11
T0931	1300	8–11
	900	6–9
T0932	1200	7–12
T0933	800	9–11
	1300	14
T0935	1300	7–15
	1400	9–11

(JEOL JXA-8900RL), transmission electron microscopy (Philips CM20 FEG scanning TEM operating at 200 kV), and Raman spectroscopy (Renishaw RM-1000).

RESULTS AND DISCUSSION

In situ observations

Several experiments were performed following different *P-T* trajectories (e.g., Fig. 3). Generally, our strategy was to pressurize the sample to ~8 GPa, a pressure where magnetite was known to remain stable from previous experiments (Schollenbruch et al. 2009) and then heat to a target temperature. Once at high temperature, the load in the hydraulic ram was again changed in steps with the resulting change in pressure monitored by measuring the unit-cell parameter of the MgO standard adjacent to the sample. In this way, pressure could be effectively increased or decreased while at high temperature. Diffraction patterns of the Fe_3O_4 sample were collected both during changes in ram load and once pressure had stabilized at a new value. Thus, we could follow the dynamic response of the sample during a change in pressure and assess how the sample behaved under new *P-T* conditions.

In experiment T0933, at 9.5 GPa and 800 °C, new diffraction peaks (*d*-spacings at 1.846, 1.43, and 1.18 Å) appeared, which are attributable to h-Fe_3O_4. The first appearance of h-Fe_3O_4 was also marked by a decrease in intensity of the diffraction peaks from magnetite. Diffraction patterns collected in a time series over several minutes revealed that some peaks of either h-Fe_3O_4 or magnetite would grow in intensity and then diminish, only to change intensity at a later point in time (Fig. 4, pattern D–F). Similar behavior was reported by Haavik et al. (2000) during their room-temperature measurements using a diamond anvil cell and an image plate detector. They suggested that this could also be due to atom motion or lattice strain, which reduces long-range order and thus reduces the sample's ability to diffract radiation. Although these effects could indeed be operative, our observations suggest that a combination of grain growth and changing grain orientation in the sample during the phase transition also play important roles. This is especially the case when using a fixed energy-dispersive detector and a narrow beam diameter (~100 µm in linear dimension), which may only illuminate a relatively small number of grains at any one time. Only after a further step in pressure did the h-Fe_3O_4-related diffraction peaks become more numerous and intense. The same type of behavior was also observed in experiment T0935 at 1300 °C once reaching a pressure of ~10.5 GPa. In these two experiments, as well as in experiment T0932, the phase transformation was accompanied by a constant pressure or a small drop in pressure even though the ram load was increased constantly (see Fig. 3). This could reflect pressure buffering since the volume change of the magnetite to h-Fe_3O_4 transition is ~ –6.5% (Fei et al. 1999). Thus as h-Fe_3O_4 is formed, the sample volume decreases causing a local lowering of pressure, which temporarily re-stabilizes magnetite and drives the reverse reaction.

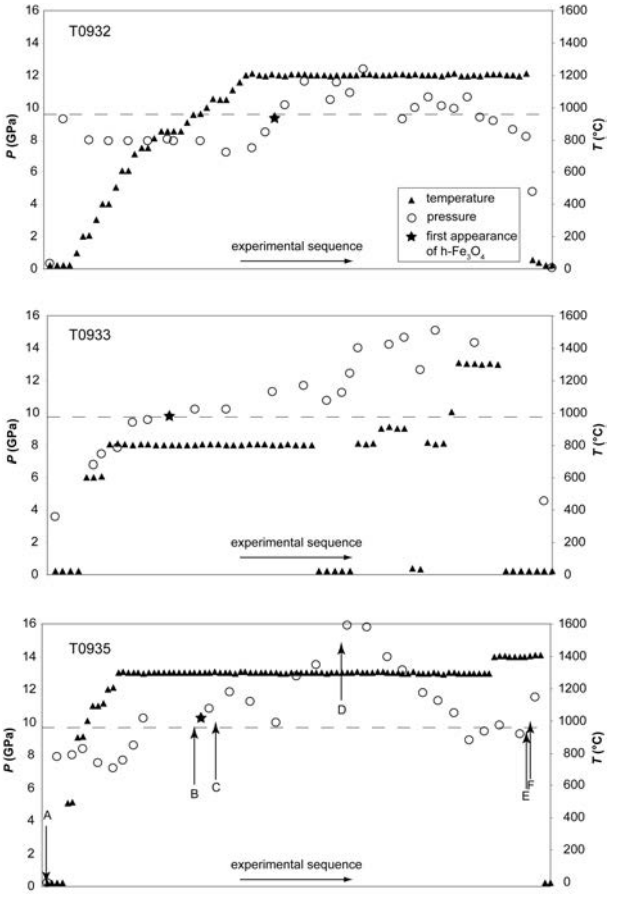

FIGURE 3. Pressure (GPa) and temperature (°C) trajectory of experiments T0932, T0933, and T0935. Dashed line denotes the position of the phase boundary. The letters represent the measurements illustrated in Figure 4. The star refers to the first appearance of h-Fe_3O_4 in each of the experiments.

The intensities of the h-Fe_3O_4 reflections increased with further increases in pressure. However, complete transformation to single-phase h-Fe_3O_4 was never attained, even after reaching 16 GPa at 1300 °C (Fig. 4). A reversal of the transition was performed at 1300 °C by progressively reducing pressure from 16 to 8 GPa. The same type of low-intensity diffraction pattern described previously was observed in a narrow pressure range approaching the phase boundary (Fig. 4). Finally, at ~10 GPa, all the h-Fe_3O_4 diffraction peaks disappeared and only magnetite was present. This sample was further heated to 1400 °C and repressurized, with reflections from h-Fe_3O_4 appearing once again at ~9.5 GPa. In total, the magnetite–h-Fe_3O_4 phase boundary was intersected at 700, 800, 1200, 1300, and 1400 °C (Table 2). Over this temperature range of 700 °C, the diffraction peaks of h-Fe_3O_4 always appeared between ~9 and ~11.5 GPa implying a nearly isobaric phase boundary.

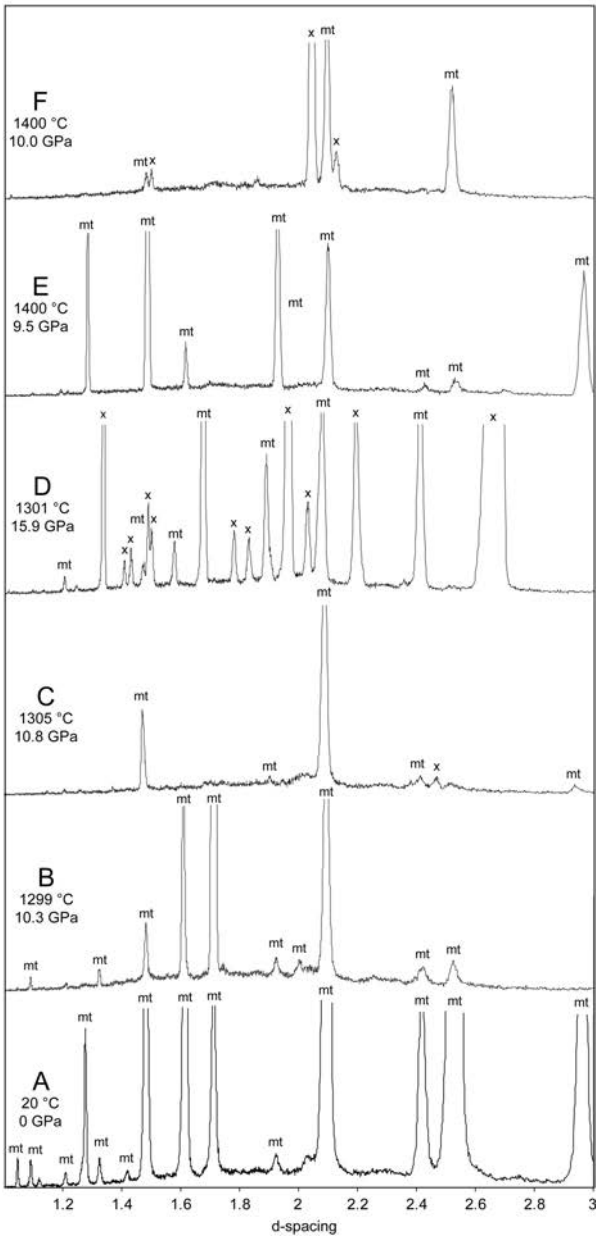

FIGURE 4. Phase development during experiment T0935. Note that A–F represents a time series. A = start of the experiment, only magnetite. B = change in peak intensities, but no additional peaks. C = first appearance of h-Fe_3O_4. D = maximum pressure, still magnetite peaks present. E = below 10 GPa only magnetite peaks. F = first reappearance of h-Fe_3O_4. G = last measurement at room temperature, possible hematite formation. Abbreviations: mt = magnetite; x = h-Fe_3O_4; hem = hematite.

TABLE 2. *P* and *T* of the first emergence of h-Fe_3O_4 peaks

Experiment	*T* (°C)	Unit cell (MgO) (Å)	Pressure* (GPa)
T0930	800	4.1704(6)	9.5 ± 0.6
T0931	700	4.1496(3)	9.3 ± 0.6
T0932	1200	4.1852(6)	11.6 ± 0.8
T0933	800	4.1707(2)	9.0 ± 0.6
T0935a	1300	4.1854(4)	10.8 ± 0.8
T0935b	1400	4.2033(7)	10.0 ± 0.9

* Pressure and error range are calculated on the basis of the EoS for MgO from Dewaele et al. (2000).

Post-experiment analyses

After the experiments, the pressure cell was mounted in epoxy, cut in half and polished for study by electron microprobe. Texturally, significant grain growth was apparent, particularly around the periphery of the sample (Fig. 5). This coarsening is consistent with observations made during the acquisition of some diffraction patterns during the experiments where certain reflections exhibited unexpectedly strong intensities. Chemical analysis revealed that some reaction had occurred between the sample and the MgO sleeve, producing a Fe_3O_4-$MgFe_2O_4$ solid solution. Reaction was limited to a thin, 20–50 µm rim region and probably did not influence the diffraction patterns obtained during the experiments since the beam was centered on the sample using the imaging mode. However, inclusion of this rim in the diffraction patterns cannot completely be ruled out.

Additional phases

In two experiments (T0930, T0935), a few hematite grains were observed by microprobe analysis. In T0930 the amount of hematite remained below the resolution of the X-ray diffraction patterns, whereas in T0935 the first hematite peaks appeared during the last stage of the experiment, during heating to 1400 °C and pressurizing above 10 GPa. No hematite was detected in the other experiments.

The h-Fe_3O_4 phase

Unfortunately, the nature of diffraction patterns collected in energy-dispersive mode does not allow an unequivocal determination of the crystal structure of h-Fe_3O_4 in our experiments. This is primarily because peak intensities are too unreliable for a proper Rietveld analysis; changing relative peak intensities due to local grain growth was observed during collection of many diffraction patterns. In addition, the apparent persistence of magnetite up to the highest pressures caused peak overlap, as did the appearance of hematite toward the end of one experiment. A prominent diffraction peak with a *d*-spacing of ~2.64 Å is observable in all patterns obtained above 10 GPa, which agrees with the highest intensity reflection reported for h-Fe_3O_4 by Fei et al. (1999). However, refinements of the best-resolved

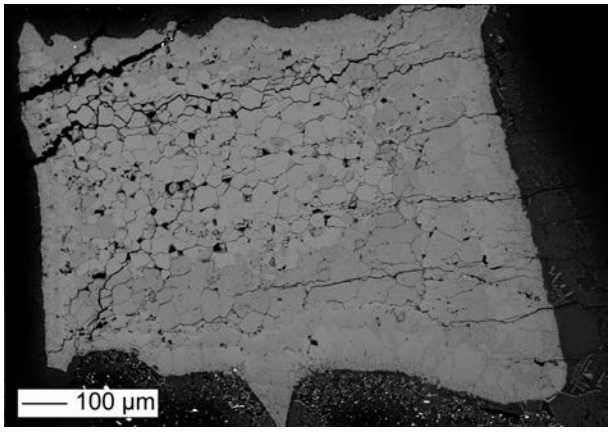

FIGURE 5. BSE photograph of a recovered sample. On the right rim Fe was incorporated in the MgO sleeve material. On the bottom, Pt grains mixed with the MgO pressure standard are visible.

diffraction patterns that were dominated by the h-Fe_3O_4 phase revealed that neither of the recently proposed structures, the $CaTi_2O_4$-type (Haavik et al. 2000; Dubrovinsky et al. 2003) or the $CaMn_2O_4$-type (Fei et al. 1999), was consistent with the set of reflections observed in our experiments. Although several peaks are indeed consistent with the $CaMn_2O_4$ structure (e.g., the strongest peak at d = 2. 624 and four other strong peaks at d = 2.040, 1.777, 1.567, and 1.405 Å), other observed peaks are not. In addition, several d-spacings expected for the $CaMn_2O_4$ structure (Fei et al. 1999) were not found in our diffraction patterns. The set of d-spacings we observed at 15.1 GPa and 1301 °C (see pattern "D" in Fig. 4) are compared with literature data for various Fe-oxide structures in Table 3.

A similar set of diffraction peaks was observed by Koch et al. (2004) in samples quenched from 9–16 GPa and 1100 °C in the system Fe_3O_4-Fe_2SiO_4-Mg_2SiO_4 (Table 3). These reflections appear to belong to a Fe_3O_4-$MgFe_2O_4$ solid solution, but could not be attributed to any known phase in this chemical system. They were unable to unequivocally determine the structure of this phase, referring to it as a "mystery phase."

Our results indicate that magnetite also transforms to this "mystery phase" and, considering previous studies performed at yet higher pressures (Fei et al. 1999; Haavik et al. 2000; Dubrovinsky et al. 2003), more than one high-P polymorph of Fe_3O_4 may exist. The occurrence of an additional high-P polymorph is also supported by electrical resistivity measurements of Xu et al. (2004) and Schollenbruch et al. (2009), who reported strong increases in resistivity for h-Fe_3O_4, in contrast to the metallic behavior observed by Dubrovinsky et al. (2003) at >24 GPa. The exact structure of this "mystery phase" awaits further investigation.

TEM observations

At the end of two experiments, the final diffraction patterns suggested the persistence of h-Fe_3O_4 at ambient conditions. In another experiment, we directly quenched our sample from 1400 °C and 11 GPa in the hope of preserving h-Fe_3O_4 for subsequent structural investigation. However, TEM investigation of these samples revealed reconversion to the spinel structure had occurred during final recovery of the sample. The magnetite was found to have numerous twins on {311} planes (Fig. 6), as is obvious from high-resolution TEM images and electron diffraction patterns. Thereby, the [110]* directions of twins are rotated by 62° with respect to the host lattice. Such a twin law is so far not known for magnetite. The lamellar to needle-like shape of the twins suggests that they may be caused by a transformation from a high-symmetry phase to one with a lower symmetry, as could happen during the transformation of cubic

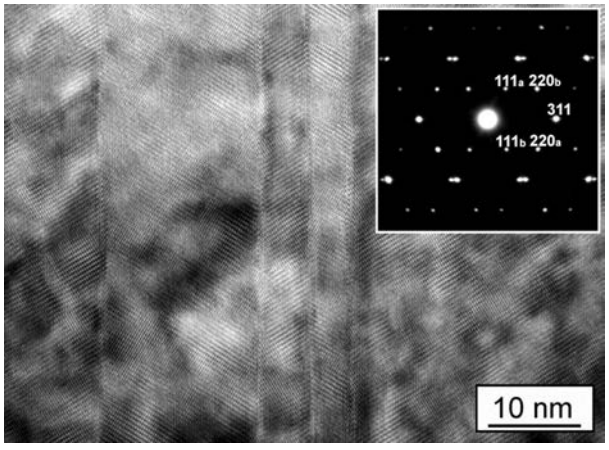

FIGURE 6. High-resolution TEM image and corresponding selected area electron diffraction pattern of magnetite recovered from run TO933. Both images reveal the presence of multiple twins parallel to the (311) plane. The zone axes of host magnetite and twins are $[\bar{1}12]$ and $[1\bar{1}\bar{2}]$, respectively.

TABLE 3. d-values (in angstroms) of our h-Fe_3O_4 phase compared with other Fe-oxide structures

h-Fe_3O_4 at 15.1 GPa and 1301 °C (this study)	"mystery phase" at 0 GPa and RT (Koch et al 2004)	h-Fe_3O_4 at 24 GPa and 650 °C (Fei et al. 2000)*	h-Fe_3O_4 at 25 GPa and RT (Mao et al. 1974)	Hematite at 0 GPa and RT (JCPDS file 33-664)	Magnetite at 0 GPa and RT (Fleet 1984)
	4.705 (4)			4.848 (10)	
				3.684 (30)	
		3.340 (3)			2.9688 (30)
	2.708 (28)	2.683 (10)		2.700 (100)	
2.670					
2.643	2.643 (100)	2.624 (100)			
		2.582 (34)	2.60 (10)	2.519 (7)	2.5317 (100)
2.409 (?)	2.444 (24)		2.44 (1)		2.424 (8)
	2.236 (15)	2.352 (14)	2.35 (3)	2.292 (3)	
2.195	2.133 (33)	2.335 (18)		2.207 (20)	
		2.117 (8)	2.14 (1)	2.0779 (3)	2.0992 (20)
2.031	2.046 (54)	2.040 (27)	2.03 (4)		
1.964		1.911 (29)			
1.889		1.887 (2)	1.90 (4)	1.8406 (40)	
1.829					
1.780		1.777 (12)	1.79 (2)	1.6941 (45)	1.714 (9)
	1.672 (9)			1.6033 (5)	1.6160 (28)
1.577	1.570 (15)	1.581 (14)		1.5992 (10)	
	1.512 (11)	1.567 (20)			
1.501	1.507 (12)	1.549 (7)	1.55 (4)	1.4859 (30)	
1.430	1.448 (10)	1.541 (17)		1.4538 (30)	1.4844 (37)
1.408		1.405 (14)	1.40 (5)	1.3497 (3)	
1.336		1.400 (8)		1.3115 (10)	1.3277 (3)
		1.312 (8)		1.3064 (6)	1.2805 (7)
		1.235 (16	1.23 (1)	1.2592 (8)	1.2659 (3)
1.18		1.203 (6)		1.2278 (4)	1.2120 (2)

Note: Where available, the numbers in parentheses represent the relative intensities.
* Calculated with XPow (Downs et al. 1993).

magnetite to orthorhombic h-Fe_3O_4. Such microstructures have also been found in magnetite samples recovered from normal quench experiments (Frost et al. 2001) and after in situ electrical resistivity measurements at high pressures and temperatures (Schollenbruch et al. 2009), and were likewise considered to indicate the magnetite to h-Fe_3O_4 transition. This interpretation was further supported by the absence of such microstructures in the starting material and in samples from experiments performed at ≤9 GPa (Schollenbruch et al. 2009), which argues against them being deformation twins. Considering that the samples investigated in this study are known to have contained h-Fe_3O_4 during the experiments, we are able to unequivocally confirm the link between the formation of these microstructures and the magnetite to h-Fe_3O_4 transition. Whether the twins actually formed during the transition from magnetite to the lower symmetric h-Fe_3O_4 or during the reverse reaction forming magnetite upon decompression remains open. In the later case, twins could develop in magnetite if there was more than one transformation path from the h-Fe_3O_4 to the spinel structure. In principle, such extensive twinning should cause certain diffraction peaks to exhibit significant broadening, reflecting the structural repeat in a particular crystallographic direction. However, we find no convincing evidence for selective peak broadening either in the set of diffraction peaks attributable to h-Fe_3O_4 or in the magnetite that formed upon decompression (e.g., see Fig. 4).

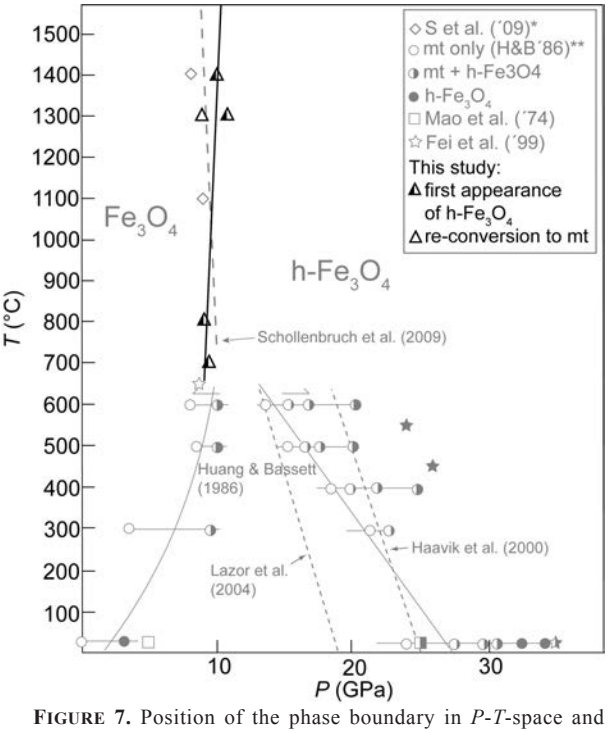

FIGURE 7. Position of the phase boundary in *P*-*T*-space and comparison with literature data. Open symbols represent the stability of magnetite, solid symbols stand for the stability of h-Fe_3O_4 and half-filled symbols the coexistence of magnetite + h-Fe_3O_4. * = Schollenbruch et al. (2009), ** = Huang and Bassett (1986). Note: literature data presented in gray to highlight this study.

The transition

A major goal of this study was to investigate the nature of the transformation of magnetite to its high-*P* polymorph and to determine the position of the phase boundary. At room temperature, magnetite has been observed to coexist with h-Fe_3O_4 at pressures up to 60 GPa (Dubrovinsky et al. 2003; Pasternak et al. 1994). Experiments by Huang and Bassett (1986) and Woodland et al. (2001) also indicated magnetite coexisting with h-Fe_3O_4 over a significant pressure interval, even at moderate temperatures (Fig. 7). Likewise, the reversion of h-Fe_3O_4 to magnetite was considered to be sluggish as well (Huang and Bassett 1986). Our in situ experiments at >1000 °C were intended to overcome the apparent hysteresis in the reaction kinetics encountered at lower temperatures. However, even at 1300 °C and 16 GPa significant amounts of magnetite were present in diffraction patterns, even after remaining at these conditions for 30 min (see pattern D in Fig. 4). On the other hand, h-Fe_3O_4 disappears quite readily during pressure release, suggesting the reverse reaction to magnetite is rather rapid.

The observed low-intensity nature of diffraction patterns collected during crossing of the phase boundary both during pressure increase and pressure release suggests that nucleation and growth are important mechanisms for the transition. However, this behavior occurs over a very large temperature range, implying that athermal processes are also involved. The persistence of magnetite coexisting with h-Fe_3O_4 even at high temperatures also points to athermal processes being important (i.e., a diffusionless transformation mechanism), although this could potentially be due to incorporation of Mg in the spinel phase, which would increase its stability. Chen et al. (2001) proposed that the olivine-spinel transition in fayalite is of a pseudomartensitic type, where the oxygen sublattice remains essentially stationary and the cations undergo short-range diffusional reordering. This mechanism is also partly related to that recently proposed for the transition in $CdCr_2O_4$ spinel at high pressures and temperatures (Arévalo-López etal. 2010). For this spinel, a two-stage process was proposed with an intermediate structure formed by cation diffusion across shared edges of octahedra (i.e., short-range reordering), followed by a reconstructive reorganization of the new octahedra to produce the $CaFe_2O_4$-type structure. Such types of transformation mechanisms could also be operative in the case of magnetite and would be consistent with our observations that point to elements of both diffusional as well as diffusionless mechanisms. Such a transformation would still be stress-sensitive, hence the appearance of more and stronger reflections from h-Fe_3O_4 during subsequent pressure increases (at constant *T*). However, since our energy-dispersive diffraction patterns preclude rigorous refinement, we are unable to directly test this hypothesis presently. This is further complicated by the fact that the exact crystal structure of h-Fe_3O_4 remains unknown, making discussion of possible displacement vectors premature. However, it is likely that the oxygen sublattices in two oxide phases like magnetite and h-Fe_3O_4 can be related through some displacement vector or vectors. These conclusions are consistent with earlier in situ observations made at lower temperatures (600–800 °C) using an externally heated diamond anvil cell and an image plate collector that allowed better quality diffraction patterns to be obtained (Woodland et al. 2001). In this study, broadening of the magnetite diffraction peaks was found to occur when coexisting with h-Fe_3O_4. The peak broadening was also reversible and dis-

appeared once h-Fe_3O_4 became unstable during decompression at pressures below 10 GPa. This behavior was interpreted as indicating that the phase transition is coherent or semi-coherent in nature and causes strain in the magnetite structure when h-Fe_3O_4 begins to form (Woodland et al. 2001). It should be noted that in these experiments no Mg was present, precluding the possibility that a $MgFe_2O_4$ component in magnetite caused the persistence of this phase to higher pressures.

The phase boundary

Based upon the kinetic behavior described above, we chose to define the position of the phase boundary by the first appearance of diffraction peaks belonging to h-Fe_3O_4 when increasing pressure from within the magnetite stability field. In our five experiments, we were able to observe the appearance of h-Fe_3O_4 diffraction peaks at 700 °C and 9.3 GPa, 800 °C and 9.5 GPa (9.0 GPa), 1200 °C and 11.6 GPa, 1300 °C and 10.8 GPa, and at 1400 °C and 10 GPa (Table 2). During experiment T0935, pressure was also decreased while at 1300 °C (see Fig. 3). Nearly immediately upon reaching ~10 GPa the diffraction peaks from h-Fe_3O_4 disappeared and magnetite reflections grew in intensity. This provides a rather tight reversal for the appearance and disappearance of h-Fe_3O_4 at 1300 °C. In addition, results from the recent resistivity experiments of Schollenbruch et al. (2009) provide further information concerning the position of the phase boundary. These experiments followed the *P-T* path marked "A" and "A'" in Figure 1 and an experiment at 9 GPa revealed that magnetite was stable up to 1400 °C, with no evidence for h-Fe_3O_4 having formed. Our experimental results place constraints on the position of the magnetite-h-Fe_3O_4 phase boundary that span 700° and indicate that it is nearly isobaric (Fig. 7). These constraints yield the following estimate for the position of the phase boundary:

$$P\,(\text{GPa}) = 1.5 \times 10^{-3}\,T\,(\text{K}) + 8.0.$$

At this point, a rigorous assessment of the uncertainties in the slope of the phase boundary is compromised by (1) the low-intensity diffraction patterns obtained at conditions near the boundary, (2) the variably sized pressure steps during the experiments, and (3) uncertainties related to using the EoS of MgO as a pressure monitor (see Dewaele et al. 2000). A qualitative assessment suggests an overall uncertainty in the position of the phase boundary of ~1 GPa. However, the appearance of h-Fe_3O_4 at slightly higher pressures at 1400 and 1300 °C compared to that at 700 and 800 °C does indeed imply that the boundary has a slightly positive d*P*/d*T* slope (Fig. 7). The results of the resistivity study of Schollenbruch et al. (2009) are consistent with our phase boundary within the uncertainties of pressure measurement; no h-Fe_3O_4 was present at 9 GPa, but it appeared in the experiment at 10 GPa. The temperature at which h-Fe_3O_4 first appeared in the latter experiment was no doubt controlled by the different *P-T* trajectory of the experiment (Fig. 1), the heating rate and the slower reaction kinetics at lower temperatures.

The fact that the structure of h-Fe_3O_4 remains to be resolved means that we are currently unable to determine the phase's molar volume, which precludes meaningful thermodynamic analysis of this transformation. Qualitatively, the nearly isobaric nature of the boundary indicates that the ΔV of the transformation is the deciding factor in driving the reaction. The slightly positive slope of the boundary implies that the entropy change of this reaction must also be negative.

Our observations on the nature of the transition suggest that the kinetics of the reverse reaction from h-Fe_3O_4 to magnetite is more rapid than the forward reaction. Thus, the disappearance of h-Fe_3O_4 might be a more reliable indicator of the phase boundary, particularly at low temperatures, where the reaction kinetics becomes less favorable. Huang and Bassett (1986) performed several experiments in a diamond anvil cell at 300–600 °C that involved compression and decompression segments. During their decompression segment, they found that h-Fe_3O_4 disappeared at pressures below 10 GPa. Fei et al. (1999) also observed that h-Fe_3O_4 had completely reacted to magnetite at 650 °C and ~9 GPa. Our preferred position for the phase boundary is consistent with these results (Fig. 7).

Several in situ studies performed at room temperature suggested the phase boundary to lie at 19–25 GPa and to have a strongly negative d*P*/d*T* slope (Lazor et al. 2004; Haavik et al. 2000). Extrapolation of these results to higher temperatures reveals that they are inconsistent with our observations (Fig. 7). The most obvious explanation for this is that these authors based the position of their boundary for the most part on the first appearance of h-Fe_3O_4 and a significant overstep in pressure was necessary to nucleate the high-pressure phase at such low temperatures. Similar behavior was observed by Zhang et al. (1996) for the coesite–stishovite transition, where slow kinetics at low temperatures suggested a negative *P-T* slope, but a definitely positive slope was apparent from measurements made above 1000 °C. Based upon a thermodynamic analysis, Lazor et al. (2004) also proposed that magnetite breaks down to a mixture of FeO and Fe_2O_3 before converting to h-Fe_3O_4 at higher pressures. Their theoretical stability field for FeO + Fe_2O_3 pinches out at ~580 °C and above this temperature magnetite should transform directly to h-Fe_3O_4. Considering the unfavourable kinetics of this system, it is questionable whether the existence of a FeO + Fe_2O_3 stability field can be reliably tested experimentally. However, we note that the position of our phase boundary lies at lower pressures than the stability field for FeO + Fe_2O_3 proposed by Lazor et al. (2004), indicating that their assumptions related to the thermodynamic properties of h-Fe_3O_4 require reassessment. No evidence of FeO was ever observed in any diffraction pattern acquired during our experiments, even those where hematite reflections were present. This further suggests that minor oxidation caused progressive formation of hematite in several of our experiments. However the amount of hematite was very small and only unambiguously detectable during microprobe analysis after the experiments.

IMPLICATIONS

Although our diffraction data for h-Fe_3O_4 do not permit an unambiguous refinement of its crystal structure at this time, the apparent discovery of a post-spinel polymorph of Fe_3O_4 additional to those previously proposed (e.g., Fei et al. 1999; Haavik et al. 2000; Dubrovinsky et al. 2003), indicates the necessity for further study of the phase relations and thermodynamics in this system at high pressures and temperatures. This is particularly the case since this phase exhibits very different electronic behavior

compared to either magnetite or that reported for the $CaTi_2O_4$-structured polymorph (Schollenbruch et al. 2009; Morris and Williams 1997; Dubrovinsky et al. 2003).

Although the presence of magnetite in samples from the Earth's mantle is quite limited, its occurrence as inclusions in diamond suggests that it may play a role during diamond formation (Meyer 1987; Stachel et al. 1998; Logvinova et al. 2010). The nearly isobaric nature of the magnetite–h-Fe_3O_4 phase boundary could permit its use as an indicator of whether a diamond originated at pressures >10 GPa or not. The presence of microtwins on the (311) plane would be indicative of the grain having undergone the transition to h-Fe_3O_4. Even if the microstructures of the inclusion equilibrated on the way to the surface, it is possible that evidence for the volume increase during the reversion to magnetite would be preserved around the interface between the inclusion and the surrounding diamond. Considering that inclusions in diamond can be under significant remnant pressure (e.g., Glinnemann et al. 2003), it is also feasible that h-Fe_3O_4 could be preserved in situ in diamonds.

The study of Koch et al. (2004) indicates that the high-pressure polymorph identified here is stable in Mg-bearing compositions, also at similar pressures. However, its stability field was not defined in this system. Clearly further work is required to understand the influence of the post-spinel transition on the stabilities of solid solutions involving a Fe_3O_4 component.

Acknowledgments

This study was supported by grants from the Deutsche Forschungsgemeinschaft within the aegis of the priority program 1236 (Wo 652/9-1, FR 1555/4-1, Louisiana 830/13-1) and within the Leibniz program (LA 830/14-1). R. Angel and T. Boffa Ballaran are thanked for their help with analysis of the in situ diffraction patterns. This study benefited from numerous discussions with L. Dubrovinsky. Portions of this work were performed at GeoSoilEnviroCARS (GSECARS; Sector 13), Advanced Photon Source (APS), Argonne National Laboratory. GSECARS is supported by the National Science Foundation—Earth Sciences (EAR-0622171) and Department of Energy—Geosciences (DE-FG02-94ER14466). Use of the Advanced Photon Source was supported by the U.S. Department of Energy, Office of Science, Office of Basic Energy Sciences, under Contract No. DE-AC02-06-CH11357. H. Ohfuji (Ehime University) and an anonymous reviewer are thanked for their insightful comments.

References cited

Arévalo-López, A.M., Dos Santos-Garcia, A.J., Catillo-Martinez, E., Durán, A., and Alario-Franco, M.A. (2010) Spinel to $CaFe_2O_4$ transformation: Mechanism and properties of B-$CdCr_2O_4$. Inorganic Chemistry, 49, 2827–2833.

Chen, J.C., Weidner, D.J., Parise, J.B., Vaughn, M.T., and Raterron, P. (2001) Observation of cation reordering during the olivine-spinel transition in fayalite by in situ synchrotron X-ray diffraction at high pressure and temperature. Physical Review Letters, 86, 4072–4075.

Dewaele, A., Fiquet, G., Andrault, D., and Häusermann, D. (2000) P-V-T equation of state of periclase from synchroton radiation measurements. Journal of Geophysical Research, 105(B2), 2869–2877.

Dieckmann, R. (1982) Defects and cation diffusion in magnetite (IV)-nonstoichiometry and point-defect structure of magnetite $Fe_{3-\delta}O_4$. Berichte Der Bunsen-Gesellschaft-Physical Chemistry Chemical Physics, 86, 112–118.

Downs, R.T., Bartelmehs, K.L., Gibbs, G.V., and Boisen, M.B. (1993) Interactive software for calculating and displaying X-ray or neutron powder diffractometer patterns of crystalline materials. American Mineralogist, 78, 1104–1107.

Dubrovinsky, L.S., Dubrovinskaia, N.A., McCammon, C., Rozenberg, G.K., Ahuja, R., Osorio-Guillen, J.M., Dmitriev, V., Weber, H.P., Le Bihan, T., and Johansson, B. (2003) The structure of the metallic high-pressure Fe_3O_4 polymorph: experimental and theoretical study. Journal of Physics-Condensed Matter, 15, 7697–7706.

Fei, Y.W., Frost, D.J., Mao, H.K., Prewitt, C.T., and Häusermann, D. (1999) In situ structure determination of the high-pressure phase of Fe_3O_4. American Mineralogist, 84, 203–206.

Fleet, M.E. (1984) The structure of magnetite: two annealed natural magnetites, $Fe_{3.005}O_4$ and $Fe_{2.96}M_{0.04}O_4$. Acta Crystallographica, C40, 1491–1493.

Frost, D.J., Langenhorst, F., and van Aken, P.A. (2001) Fe-Mg partitioning between ringwoodite and magnesiowustite and the effect of pressure, temperature and oxygen fugacity. Physics and Chemistry of Minerals, 28, 455–470.

Glinnemann, J., Kusaka, K., and Harris, J.W. (2003) Oriented graphite single-crystal inclusions in diamond. Zeitschrift für Kristallographie, 218, 733–739.

Haavik, C., Stølen, S., Fjellvåg, H., Hanfland, M., and Häusermann, D. (2000) Equation of state of magnetite and its high-pressure modification: Thermodynamics of the Fe-O system at high pressure. American Mineralogist, 85, 514–523.

Huang, E. and Bassett, W.A. (1986) Rapid-determination of Fe_3O_4 phase-diagram by synchrotron radiation. Journal of Geophysical Research-Solid Earth and Planets, 91(B5), 4697–4703.

Jamieson, J.C., Fritz, J.N., and Manghnani, M.H. (1982) Pressure measurement at high temperature in X-ray diffraction studies: Gold as a primary standard. In S. Akimoto and M.H. Manghnani, Eds., High-Pressure Research in Geophysics Pressure, p. 27–48. Center for Academic Publications, Tokyo, Japan.

Koch, M., Woodland, A.B., and Angel, R.J. (2004) Stability of spinlloid phases in the system Mg_2SiO_4-Fe_2SiO_4-Fe_3O_4 at 1000 °C and up to 10.5 GPa. Physics of the Earth and Planetary Interiors, 143, 171–183.

Larson, A.C. and von Dreele, R.B. (1988) GSAS manual. Los Alamos National Laboratory, report LAUR, 86-748.

Lazor, P., Shebanova, O.N., and Annersten, H. (2004) High-pressure study of stability of magnetite by thermodynamic analysis and synchrotron X-ray diffraction. Journal of Geophysical Research-Solid Earth, 109, B05201.

Logvinova, A.M., Wirth, R., and Sobolev, N.V. (2010) Fluid/melt inclusions in alluvial Northeast Siberian diamonds: new approach on diamond formation. Geophysical Research Abstracts, 12, EGU2010-1236.

Mao, H.K., Takahash, T, Bassett, W.A., Kinsland, G.L., and Merrill, L. (1974) Isothermal compression of magnetite to 320 Kbar and pressure-induced phase-transformation. Journal of Geophysical Research, 79, 1165–1170.

Meyer, H.A.O. (1987) Inclusions in diamond. In P.H. Nixon, Ed., Mantle Xenoliths, p. 501–522. Wiley, New York.

Morris, E.R. and Williams, Q. (1997) Electrical resistivity of Fe_3O_4 to 48 GPa: Compression-induced changes in electron hopping at mantle pressures. Journal of Geophysical Research-Solid Earth, 102, 18139–18148.

O'Neill, H.St.C., Rubie, D.C., Canil, D., Geiger, C.A., Ross, C.R. II, Seifert, F., and Woodland, A.B. (1993) Ferric iron in the upper mantle and in transition zone assemblages: implications for relative oxygen fugacities in the mantle. In Geophysical Monograph 74, IUGG vol. 14, p. 73–88. American Geophysical Union, Washington D.C.,

Pasternak, M.P., Nasu, S., Wada, K., and Endo, S. (1994) High-pressure phase of magnetite. Physical Review B, 50, 6446–6449.

Schollenbruch, K., Woodland, A.B., Frost, D.J., and Langenhorst, F. (2009) Detecting the spinel-post-spinel transition in Fe_3O_4 by in situ electrical resistivity measurements. High Pressure Research, 29, 520–524.

Stachel, T., Harris, J.W., and Brey, G.P. (1998) Rare and unusual mineral inclusions in diamonds from Mwadui, Tanzania. Contributions to Mineralogy and Petrology, 132, 307–307.

Toby, B.H. (2001) EXPGUI, a graphical user interface for GSAS. Journal of Applied Crystallography, 34, 210–213.

Wang, Y., Rivers, M., Sutton, S., Eng, P., Shen, G., and Getting, I. (1998) A multi-anvil, high-pressure facility for synchroton radiation research at GeoSoilEnviroCars at the advanced photo source. The Review of High Pressure Science and Technology, 7, 1490–1495.

Wang, Y., Rivers, M., Sutton, S., Nishiyama, N., Uchida, T., and Sanehira, T. (2009) The large-volume high pressure facility at GSECARS: A "Swiss-army-knife" approach to synchroton-based experimental studies. Physics of the Earth and Planetary Interiors, 174, 270–281.

Wood, B.J. and Virgo, D. (1989) Upper mantle oxidation state: Ferric iron contents of lherzolite spinels by ^{57}Fe Mössbauer spectroscopy and resultant oxygen fugacities. Geochimica et Cosmochimica Acta, 53, 1277–1291.

Woodland, A.B., Angel, R.J., Frost, D.J., and Koch, M. (2001) Determination of the post-spinel phase boundary in magnetite and Si-bearing spinel at high pressures and temperatures. ESRF Report HS1214, European Synchrotron Radiation Facility, Grenoble, France.

Xu, W.M., Machavariani, G.Y., Rozenberg, G.K., and Pasternak, M.P. (2004) Mössbauer and resistivity studies of the magnetic and electronic properties of the high-pressure phase of Fe_3O_4. Physical Review B, 70, 174106, DOI: 10.1103/PhysRevB.70.174106.

Zhang, J., Li, B., Utsumi, W., and Liebermann, R.C. (1996) In situ X-ray observations of the coesite-stishovite transition: reversed phase boundary and kinetics. Physics and Chemistry of Minerals, 23, 1–10.

Manuscript received July 5, 2010
Manuscript accepted January 6, 2011
Manuscript handled by Jennifer Kung